

Nobuo Ishizawa,^{a*} Keishi Hiraga,^a Douglas du Boulay,^a Hisashi Hibino,^a Takashi Ida^a and Shuji Oishi^b

^aCeramics Research Laboratory, Nagoya Institute of Technology, 10-6-29 Asahigaoka, Tajimi, Gifu 507-0071, Japan, and ^bDepartment of Environmental Science and Technology, Faculty of Engineering, Shinshu University, Wakasato, Nagano 380-8553, Japan

Correspondence e-mail: ishizawa@nitech.ac.jp

Key indicators

Single-crystal X-ray study
T = 293 K
Mean $\sigma(\text{Ru}-\text{O}) = 0.009 \text{ \AA}$
R factor = 0.047
wR factor = 0.035
Data-to-parameter ratio = 30.4

For details of how these key indicators were automatically derived from the article, see <http://journals.iucr.org/e>.

A non-centrosymmetric polymorph of Gd_3RuO_7

A new non-centrosymmetric modification has been found for trigadolinium ruthenium heptaoxide, Gd_3RuO_7 , crystallizing in the space group $P2_1nb$. The structure is composed of infinite single chains of corner-linked $[\text{RuO}_6]$ octahedra embedded in the $[\text{Gd}_3\text{O}]$ matrix. The octahedra in the $P2_1nb$ modification have two tilt systems about the a and c axes, in contrast to the previously reported $Cmcm$ modification [Bontchev *et al.* (2000). *Phys. Rev. B*, **62**, 12235–12240], with only one tilt system about the a axis. Changes in the coordination of Gd atoms in the title compound are closely related to the tilting mechanism about the c axis.

Received 14 November 2005

Accepted 7 December 2005

Online 14 December 2005

Comment

A series of Ln_3MO_7 crystals composed of a trivalent lanthanide (Ln) and pentavalent transition metal (M) oxides is structurally characterized by the presence of infinite single chains of corner-linked $[\text{MO}_6]$ octahedra embedded in the matrix of Ln and O atoms. This series has attracted attention in recent decades because of its interesting electrical and magnetic properties.

Single crystals of Gd_3RuO_7 , a member of the Ln_3MO_7 series, were grown by Bontchev *et al.* (2000) and reported to crystallize in the orthorhombic space group $Cmcm$ at room temperature. The electric conductivity measurement of the Gd_3RuO_7 ceramic sample revealed the Mott variable-range

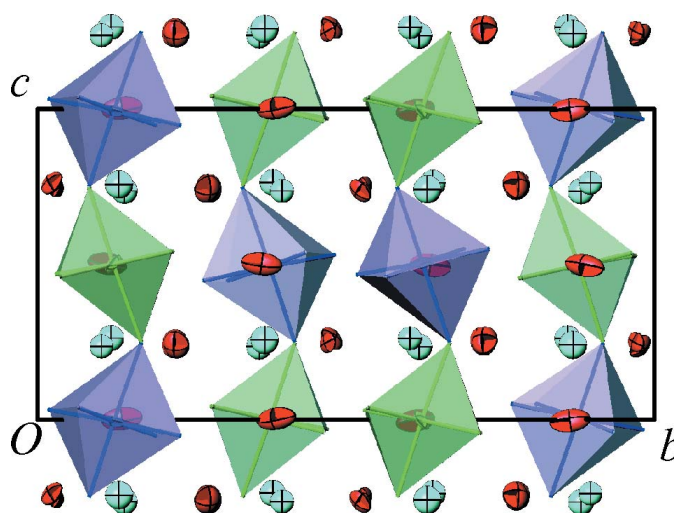


Figure 1

Structure of the $P2_1nb$ modification of Gd_3RuO_7 viewed along the a axis. Ligands of the Ru1O_6 (light purple) and Ru2O_6 (light green) octahedra are not shown for clarity. The anisotropic displacement parameters of Gd (red), Ru1 (blue) and Ru2 (green) are drawn at the 99% probability level; isotropic displacement parameters of O atoms are drawn at the same level and are given in light blue.

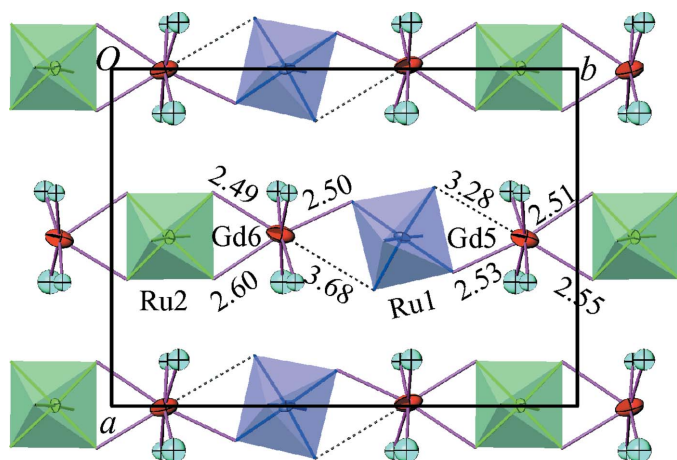


Figure 2
Slices of the $P2_1nb$ modification near the (002) plane with selected Gd—O bond distances. Colour scheme is the same as in Fig. 1.

hopping conduction of localized carriers along the $[\text{RuO}_6]$ chains (Bontchev *et al.*, 2000). Harada & Hinatsu (2002) reported the first-order phase transition of Gd_3RuO_7 at 382 K in addition to low-temperature transitions at 9.5 and 15 K. They also suggested a possible appearance of a monoclinic modification below 382 K for Gd_3RuO_7 . In the course of a systematic study of the Ln_3RuO_7 series, we encountered a new polymorph of Gd_3RuO_7 , which is neither the orthorhombic $Cmcm$ modification nor the predicted monoclinic one. It crystallizes in the non-centrosymmetric space group $P2_1nb$ with a doubled b axis compared with that of the $Cmcm$ modification.

The structure of the $P2_1nb$ modification comprises two crystallographically independent Ru atom sites, Ru1 and Ru2, whereas there is only one Ru site in the $Cmcm$ modification. The $[\text{Ru}_1\text{O}_6]$ and $[\text{Ru}_2\text{O}_6]$ octahedra are connected with each other by sharing corners to form isolated single chains along the c axis, as shown in Fig. 1. The $[\text{RuO}_6]$ octahedra are tilted about the a axis with an $\text{Ru}_1\text{—O}_1\text{—Ru}_2$ angle of $144.1(6)^\circ$ and an $\text{Ru}_1\text{—O}_2\text{—Ru}_2$ angle of $140.2(6)^\circ$, resulting in two different Ru1—Ru2 intermetallic distances of 3.632 (3) and 3.752 (3) Å, respectively. The mean values are very close to those (142.6° and 3.690 Å) reported for the $Cmcm$ modification. In the $P2_1nb$ modification, however, another tilt system exists and distinguishes the two modifications. This second tilt occurs only in $[\text{Ru}_1\text{O}_6]$ octahedra with a magnitude of approximately 13° about the axes close to the c direction. $[\text{Ru}_2\text{O}_6]$ has no such tilt system. The second tilt clearly breaks the pseudo-mirror planes at $x \simeq 0$ and $\frac{1}{2}$, excluding the possibility of the centrosymmetric space group $Pmnb$ for the present polymorph.

The Ru—O bond lengths of the $[\text{RuO}_6]$ octahedron in the $Cmcm$ modification do not differ significantly (*viz.* $1.948 \text{ \AA} \times 2$ along the chain and $1.940 \text{ \AA} \times 4$ for the others). This high regularity breaks down in the $P2_1nb$ modification. Here the Ru—O bond lengths of the double-tilted $[\text{Ru}_1\text{O}_6]$ octahedron are grouped into three (*viz.* $\sim 1.90 \text{ \AA} \times 2$, $\sim 1.95 \text{ \AA} \times 2$ and $\sim 2.01 \text{ \AA} \times 2$), while those of the single-tilted $[\text{Ru}_2\text{O}_6]$ octa-

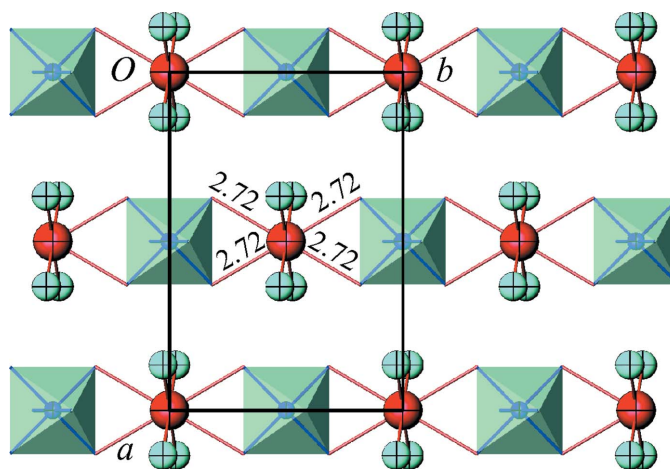


Figure 3
Slices of the $Cmcm$ modification near the (002) plane with selected Gd—O bond distances. Colour scheme is the same as in Fig. 1.

hedron are grouped into two (*viz.* $\sim 1.92 \text{ \AA} \times 3$ and $\sim 1.98 \text{ \AA} \times 3$). The splitting of the Ru—O bond lengths suggests that the energy level degeneracy of Ru is removed considerably in the $P2_1nb$ modification compared with that in $Cmcm$.

The title compound contains six crystallographically independent Gd atoms coordinated by seven O atoms each, with interatomic distances ranging from 2.190 (13) to 2.605 (13) Å (Table 1). Atoms Gd1, Gd2, Gd3 and Gd4 are related to the Gd2 site in the $Cmcm$ modification, while atoms Gd5 and Gd6 are related to the Gd1 site according to the notation given by Bontchev *et al.* (2000). The Gd1 atom in the $Cmcm$ modification has a coordination number (CN) of 8, with four short Gd—O (2.34 Å) and four long Gd—O (2.72 Å) bonds. In contrast, atoms Gd5 and Gd6 in the $P2_1nb$ modification have a CN of 7, with bond distances distributed in shorter ranges of 2.271 (12)–2.548 (12) Å for Gd5 and 2.339 (11)–2.600 (12) Å for Gd6. On the other hand, atoms Gd1, Gd2, Gd3 and Gd4 in the $P2_1nb$ modification have a CN of 7, with Gd—O bond lengths similar to those of Gd2 in the $Cmcm$ modification.

The tilting of the $[\text{Ru}_1\text{O}_6]$ octahedra about the c axis in the $P2_1nb$ modification is closely related to the coordination of Gd5 and Gd6 lying near the same (002) plane, as illustrated in Fig. 2. The dashed lines represent lengths of 3.28–3.68 Å, being much longer than the other six Gd—O bonds (three for each Gd with 2.49–2.60 Å) near the plane. On the other hand, the $[\text{RuO}_6]$ octahedra in the $Cmcm$ modification have no tilt about the c axis, as shown in Fig. 3. All four long Gd—O bonds observed in this modification lie near the (002) plane with the same length of 2.72 Å.

These facts are suggestive when one considers a possible phase transition between the $P2_1nb$ and $Cmcm$ modifications. The occurrence of octahedral tilt about the c axis in the $P2_1nb$ modification can be described by three steps: (1) systematic small displacements of atoms Gd5 and Gd6 along the direction close relative to the b axis, (2) bond breaking of Gd—O, *i.e.* $\text{Ru}_1\text{—O—Gd} \rightarrow \text{Ru}_1\text{—O}\cdots\text{Gd}$ (two breaks per $[\text{Ru}_1\text{O}_6]$ octahedron), and (3) small rotation of $[\text{Ru}_1\text{O}_6]$ octahedra about the c axis in order to balance with the two missing Gd—

O bonds near the (002) plane. These three steps are geometrically connected to each other and probably occur simultaneously in reality. Therefore it is not meaningful to insist on their sequence or the cause/effect relation. However, it is noteworthy that several different structures could be derived from the transition depending on the direction of Gd atom displacement vectors if they are energetically comparable to those that occur in the ideal $P2_1nb$ modification.

Actually we have observed rather large residual electron densities of about $\pm 17 e \text{ \AA}^{-3}$ in the direction of the b axis near atoms Gd5 and Gd6. This suggests a possible existence of local disorder of Gd atoms in the crystal structure. In addition, the structure refinement always suffered from the presence of inversion twins with nearly equal volumes. This may suggest an occurrence of systematic misorientations of the Gd displacements near the composition plane of the twins.

Bontchev *et al.* (2000) grew crystals of the $Cmcm$ modification by cooling the melt from 1573 to 1273 K at the rate of 1 K h^{-1} using the same SrCl_2 flux as we did. On the other hand, we grew the crystals by cooling the melt from 1373 to 973 K at a rate of 5 K h^{-1} with subsequent cooling in the switched-off furnace. This suggests that the present $P2_1nb$ polymorph might be a low-temperature modification with respect to the $Cmcm$ polymorph. The decrease in the CN of Gd5 and Gd6 of the $P2_1nb$ modification from 8 to 7, and a resultant shrinkage of the mean Gd—O bond length, are consistent with this assumption. Further studies to investigate the possible high temperature phase transition of the compound are in progress.

The present structure belongs to the non-centrosymmetric space group $P2_1nb$ which is polar along the a axis. The $[\text{Gd}_3\text{O}]$ matrix is supposed to be considerably insulating compared with the conductive $[\text{RuO}_6]$ chains along the c axis. Thus the crystal may be a candidate for a ferroelectric with a spontaneous polarization along the a axis.

Experimental

Crystals were grown by the flux method. The reagent grade powders of Gd_2O_3 (Wako Pure Chemical Industries Ltd., 078–04562, 3.56 mmol), RuO_2 (Japan Pure Chemical Co., 083278, 2.38 mmol) and SrCl_2 flux (Wako Wako Pure Chemical Industries, Ltd., 197–04205, 21.39 mmol) were mixed together, placed in a 30 ml platinum crucible and heated in air to 1373 K in 12 h. The crucible was then kept at that temperature for 6 h, cooled to 973 K at 5 K h^{-1} , and then cooled to room temperature in the switched-off furnace. The product was leached out with warm water to dissolve the flux. The yield was 95.7%. The crystals are black with dimensions of 10–100 μm . Most crystals grown in the present experiment had the shape of a parallelepiped prism elongated along the c axis. The side faces of the prism were composed of $\{120\}$ and the top and bottom of $\{101\}$. Considering the number and strength of bonds that intersect the crystal faces, it is reasonable to assume that the $\{120\}$ side faces are a set of planes running through the $[\text{Gd}_3\text{O}]$ matrix. No heavy elements other than Gd and Ru were found by energy dispersive spectroscopy (Jeol, JSM-6100) attached to the scanning electron microscope (JEOL, JED-2001). Most crystals had relatively high crystallinity and were identified as the $P2_1nb$ modification.

Crystal data

$\text{Gd}_3\text{O}_7\text{Ru}$
 $M_r = 684.82$
 Orthorhombic, $P2_1nb$
 $a = 10.644 (5) \text{ \AA}$
 $b = 14.685 (6) \text{ \AA}$
 $c = 7.384 (3) \text{ \AA}$
 $V = 1154.2 (9) \text{ \AA}^3$
 $Z = 8$
 $D_x = 7.882 \text{ Mg m}^{-3}$

Mo $K\alpha$ radiation
 Cell parameters from 11591 reflections
 $\theta = 3\text{--}70^\circ$
 $\mu = 36.58 \text{ mm}^{-1}$
 $T = 293 \text{ K}$
 Prism, black
 $0.10 \times 0.05 \times 0.04 \text{ mm}$

Data collection

Rigaku R-Axis RAPID image-plate diffractometer
 ω scans
 Absorption correction: numerical (*NUMABS*; Higashi, 2000)
 $T_{\min} = 0.087$, $T_{\max} = 0.183$
 95408 measured reflections

5726 independent reflections
 3921 reflections with $F > 3\sigma(F)$
 $R_{\text{int}} = 0.062$
 $\theta_{\max} = 50^\circ$
 $h = -22 \rightarrow 22$
 $k = -31 \rightarrow 31$
 $l = -15 \rightarrow 10$

Refinement

Refinement on F
 $R[F^2 > 2\sigma(F^2)] = 0.047$
 $wR(F^2) = 0.035$
 $S = 2.38$
 3921 reflections
 129 parameters
 Weighting scheme based on measured s.u.'s
 $(\Delta/\sigma)_{\max} = 0.001$

$\Delta\rho_{\max} = 17.86 e \text{ \AA}^{-3}$
 $\Delta\rho_{\min} = -17.04 e \text{ \AA}^{-3}$
 Extinction correction: Zachariasen (1967)
 Extinction coefficient: 135 (7)
 Absolute structure: Flack (1983), 3921 Friedel pairs
 Flack parameter: 0.50 (2)

Table 1

Selected bond lengths (\AA).

Gd1 ⁱ —O10 ⁱ	2.266 (14)	Gd4 ^v —O1 ⁱ	2.533 (13)
Gd1 ⁱ —O6 ⁱⁱ	2.293 (14)	Gd5—O6	2.271 (12)
Gd1 ⁱ —O13 ⁱⁱⁱ	2.318 (11)	Gd5—O8 ⁱⁱⁱ	2.296 (11)
Gd1 ⁱ —O11 ⁱ	2.334 (10)	Gd5—O10 ⁱ	2.334 (12)
Gd1 ⁱ —O9 ⁱ	2.376 (10)	Gd5—O4 ⁱⁱⁱⁱ	2.418 (11)
Gd1 ⁱ —O5 ^{iv}	2.458 (12)	Gd5—O9 ^{iv}	2.510 (10)
Gd1 ⁱ —O1 ⁱ	2.513 (13)	Gd5—O12	2.532 (11)
Gd2 ^v —O4 ^v	2.257 (13)	Gd5—O5 ^{iv}	2.548 (12)
Gd2 ^v —O8 ^{vi}	2.260 (13)	Gd6 ^{ix} —O6 ^{ix}	2.339 (11)
Gd2 ^v —O3 ⁱⁱ	2.303 (11)	Gd6 ^{ix} —O10 ⁱ	2.343 (12)
Gd2 ^v —O12 ⁱⁱ	2.381 (11)	Gd6 ^{ix} —O8 ⁱⁱⁱ	2.366 (11)
Gd2 ^v —O14 ^v	2.417 (10)	Gd6 ^{ix} —O4 ⁱ	2.368 (11)
Gd2 ^v —O2 ^v	2.444 (13)	Gd6 ^{ix} —O7 ^{ix}	2.487 (10)
Gd2 ^v —O7 ^{vii}	2.448 (10)	Gd6 ^{ix} —O11 ⁱⁱⁱ	2.500 (9)
Gd3 ⁱⁱ —O6 ⁱⁱ	2.239 (14)	Gd6 ^{ix} —O3 ^{ix}	2.600 (12)
Gd3 ⁱⁱ —O10 ⁱⁱ	2.305 (14)	Ru1 ⁱⁱⁱ —O1 ⁱⁱⁱ	1.898 (7)
Gd3 ⁱⁱ —O7 ⁱⁱ	2.350 (10)	Ru1 ⁱⁱⁱ —O14 ⁱⁱⁱ	1.902 (10)
Gd3 ⁱⁱ —O14 ⁱⁱ	2.399 (10)	Ru1 ⁱⁱⁱ —O11 ⁱⁱⁱ	1.939 (9)
Gd3 ⁱⁱ —O3 ^{iv}	2.426 (11)	Ru1 ⁱⁱⁱ —O13 ⁱⁱⁱ	1.953 (11)
Gd3 ⁱⁱ —O12 ⁱⁱⁱ	2.498 (11)	Ru1 ⁱⁱⁱ —O12 ⁱⁱⁱ	2.004 (11)
Gd3 ⁱⁱ —O2 ⁱⁱⁱ	2.605 (13)	Ru1 ⁱⁱⁱ —O2 ⁱⁱⁱ	2.008 (8)
Gd4 ^v —O4 ^v	2.190 (13)	Ru2 ^{iv} —O9 ^{iv}	1.919 (10)
Gd4 ^v —O8 ^v	2.202 (13)	Ru2 ^{iv} —O1 ^{iv}	1.920 (7)
Gd4 ^v —O13 ⁱ	2.331 (11)	Ru2 ^{iv} —O5 ^{iv}	1.924 (12)
Gd4 ^v —O5 ⁱ	2.378 (11)	Ru2 ^{iv} —O3 ^{iv}	1.977 (11)
Gd4 ^v —O9 ^{vii}	2.401 (10)	Ru2 ^{iv} —O2 ⁱⁱⁱ	1.981 (8)
Gd4 ^v —O11 ^v	2.496 (9)	Ru2 ^{iv} —O7 ^{iv}	1.982 (10)

Symmetry codes: (i) $x + \frac{1}{2}, -y + \frac{1}{2}, z + \frac{1}{2}$; (ii) $x + \frac{1}{2}, -y + 1, -z$; (iii) $x, y + \frac{1}{2}, -z + \frac{1}{2}$; (iv) $x, y + \frac{1}{2}, -z - \frac{1}{2}$; (v) $x + 1, y + \frac{1}{2}, -z + \frac{1}{2}$; (vi) $x + 1, y + 1, z$; (vii) $x + 1, y + \frac{1}{2}, -z - \frac{1}{2}$; (viii) $x + \frac{1}{2}, -y + \frac{1}{2}, z - \frac{1}{2}$; (ix) $x, y, z + 1$.

The unit cell was chosen so that the a and c axes correspond to those of the $Cmcm$ modification given by Bontchev *et al.* (2000). This resulted in a non-standard setting of the space group $Pna2_1$ (No. 33). The superstructure reflections that double the b axis were relatively strong and easy to discern. The structure was solved by direct methods (Sheldrick, 1997). No reasonable solutions were obtained assuming the centrosymmetric space group $Pmnb$, which has the same extinction rules as the non-centrosymmetric space group $P2_1nb$.

The refinement of structure models in *Pmnb* derived from the final *P2₁nb* model converged with *R* values higher than 0.12, leaving negative or extraordinarily large ADP values for several atoms. The absence of mirror planes perpendicular to the *a* axis in the structure was justified from the octahedral tilting as discussed in the *Comment*. A stoichiometric composition was assumed in the refinement since population analysis resulted in site occupation factors of 0.96 (1)–1.03 (1) for all Gd and Ru atom sites. The *x* parameter of Ru1 was fixed at 0 to define the origin in the least-squares procedure. Refinements assuming anisotropic displacement parameters for O atoms were tried in vain. The absolute structure parameter (Flack, 1983) was refined to 0.50 (2), suggesting the presence of inversion-related twin components with nearly equal volumes in the crystal. This value did not vary significantly over several different crystals sampled from the same batch. The highest peak and the deepest hole in the final difference Fourier map are located 0.53 Å from Gd5 and 0.39 Å from Gd6, respectively.

Data collection: *RAPID-AUTO* (Rigaku, 1999); cell refinement: *RAPID-AUTO*; data reduction: *Xtal3.7.2 DIFDAT SORTRF* and

ADDREF (Hall *et al.*, 2003); program(s) used to solve structure: *SHELXS97* (Sheldrick, 1997); program(s) used to refine structure: *Xtal3.7.2 CRYLSQ*; molecular graphics: *ATOMS* (Dowty, 2005); software used to prepare material for publication: *Xtal3.7.2 CIFIO*.

References

- Bontchev, R. P., Jacobson, A. J., Gospodinov, M. M., Skumryev, V., Popov, V. N., Lorenz, B., Meng, R. L., Litvinchuk, A. P. & Iliev, M. N. (2000). *Phys Rev. B*, **62**, 12235–12240.
- Dowty, E. (2005). *ATOMS for Windows*. Version 6.2. Shape Software, 521 Hidden Valley Road, Kingsport, TN 37663, USA.
- Flack, H. D. (1983). *Acta Cryst. A* **39**, 876–881.
- Hall, S. R., du Boulay, D. & Olthof-Hazekamp, R. (2003). Gnu *Xtal*. System 3.7.2. University of Western Australia, Australia.
- Harada, D. & Hinatsu, Y. (2002). *J. Solid State Chem.* **164**, 163–168.
- Higashi, T. (2000). *NUMABS*. Rigaku Corporation, Tokyo, Japan.
- Rigaku (1999). *RAPID-AUTO*. Manual No. MJ13159A01. Rigaku Corporation, Tokyo, Japan.
- Sheldrick, G. M. (1997). *SHELXS97*. University of Göttingen, Germany.
- Zachariasen, W. H. (1967). *Acta Cryst.* **23**, 558–564.